



**AUSTRALIAN ATOMIC ENERGY COMMISSION**  
**RESEARCH ESTABLISHMENT**  
**LUCAS HEIGHTS**

**A LOW INDUCTANCE CO<sub>2</sub> TE LASER**

by

**J.E. EBERHARDT**



November 1979

ISBN 0 642 59676 X



AUSTRALIAN ATOMIC ENERGY COMMISSION  
RESEARCH ESTABLISHMENT  
LUCAS HEIGHTS

A LOW INDUCTANCE CO<sub>2</sub> TE LASER

by

J.E. Eberhardt

ABSTRACT

A carbon dioxide TE laser was constructed with a half-litre discharge volume preionised by ultraviolet emitting spark arrays. The laser provided a 6 J output pulse at 10 per cent efficiency on the 944 cm<sup>-1</sup> P20 line and, when fitted with a diffraction grating, was operated on a wide range of lines (956 cm<sup>-1</sup> P4, 2J; 1017 cm<sup>-1</sup> P50, 0.5 J).

Tests showed that a uniform output flux was available from the laser before organic dopant had been used. However, raising the discharge circuit inductance from 150 nH to 1300 nH greatly disturbed the output beam uniformity by streamer growth. No significant pulse energy decrease accompanied this growth.

(Continued)

Although the average intracavity energy flux was only  $3 \text{ J cm}^{-2}$  the diffraction grating was irreparably damaged after 3/4 million shots and it was concluded that when higher fluxes are required an oscillator/amplifier approach should be considered.

Slight organic doping greatly reduces the streamer growth in high inductance discharges and its use would allow high inductance loops to be used, reducing sparkgap wear at the expense of contamination of the optics.

## CONTENTS

1. INTRODUCTION	1
2. LASER CONSTRUCTION	2
2.1 Laser Box	3
2.2 Rogowski Electrodes	3
2.3 Preionisation Arrays	4
2.4 Brewster Window Holder	4
3. DISCHARGE CIRCUITS	4
3.1 Preionisation Circuit	5
3.2 Main Discharge Circuit	6
3.3 Triggered Sparkgaps	7
3.4 Trigger Generation	8
4. THE OPTICAL CAVITY	9
4.1 Output Pulse Shape	10
4.2 Beam Characteristics and Wavelength Range	10
4.3 Far Field Flux Density	11
4.4 Inductance and Beam Uniformity	11
5. GAS HANDLING	12
5.1 Mixture Optimisation	12
5.2 Gas Impurities	13
5.3 Gas Additives	14
6. MAINTENANCE	15
7. CONCLUSIONS	16
8. ACKNOWLEDGEMENT	17
9. REFERENCES	17

(Continued)

## CONTENTS (Continued)

Table 1 Wavelength Range	21
Figure 1 Mechanical layout of laser	23
Figure 2 Rogowski $\pi/2$ electrode profile 20 mm flat, 20 mm spacing	24
Figure 3 Brewster Window Holder	25
Figure 4 UV preioniser circuit	26
Figure 5 Sidelight variation with peaking capacitor value	27
Figure 6 Main discharge circuit	27
Figure 7 Mechanical layout of main discharge circuit	28
Figure 8 Triggered spark gap with ceramic trigger insulator	29
Figure 9 Sparkgap trigger delay	30
Figure 10 Measurement configuration for flux density profiles	31
Figure 11 Far field flux density profiles	32

National Library of Australia card number and ISBN 0 642 59676 X

The following descriptors have been selected from the INIS Thesaurus to describe the subject content of this report for information retrieval purposes. For further details please refer to IAEA-INIS-12 (INIS: Manual for Indexing) and IAEA-INIS-13 (INIS: Thesaurus) published in Vienna by the International Atomic Energy Agency.

CARBON DIOXIDE LASERS; EFFICIENCY; PERFORMANCE; RELIABILITY



## 1. INTRODUCTION

For several years the Special Studies Group of the Australian Atomic Energy Commission's Instrumentation and Control Division has been engaged in research on the photo-dissociation of molecules using infrared radiation generated by pulsed CO<sub>2</sub> lasers. The pulse energy required is not large, a few joules at about 1 Hz permit a wide range of experiments requiring consistent output, in contrast to plasma diagnostic experiments where pulses of tens or hundreds of joules are needed but only several times a day.

For photo-dissociation experiments the most exacting requirements are a uniform output flux and reliable operation for many pulses. Usually the laser must provide 10 000 pulses per day and well over a million pulses per year. Some otherwise excellent commercial CO<sub>2</sub> lasers incorporate components with a service life of only 20 000 pulses which makes them unsuitable for photo-dissociation experiments.

In many applications the operating wavelength of a CO<sub>2</sub> laser is unimportant but photo-dissociation research demands that the laser be forced to operate on a single vibrational-rotational transition, selected at will from over a hundred possible transitions with wavelengths near 10 μm. Usually the selected transition provides less laser gain than the transition on which the laser would otherwise operate, and high reflectivity mirrors are required. A laser operated in this fashion produces longer and lower power pulses than does one which operates at the preferred 10.59 μm wavelength.

The outstanding characteristic of the carbon dioxide molecular laser is its efficiency. A wallplug-to-output flux efficiency of ten per cent is easily attained with a pulsed discharge in high pressure carbon dioxide, and transversely excited high pressure carbon dioxide (CO<sub>2</sub> TE) lasers are well known for their ability to produce intense infrared light pulses [Beaulieu 1970; Pearson 1972; Pan Yu-li et al. 1972; Wood 1974].

The glow discharges which are necessary to pump the carbon dioxide are unstable and tend to degenerate into inter-electrode arcs. As the carbon dioxide partial pressure is raised, the available infrared pulse energy increases but the glow-to-arc transition interval shortens until an arc occurs before the device can lase. Energy otherwise available to pump the CO<sub>2</sub> is consumed by the arc which also disrupts the optical homogeneity of the laser

gain medium. Increasing the energy input to the gas causes earlier arcing.

Many techniques have been developed to prolong the interval before arcing and increase the allowable input energy density. The most effective of these is to deposit the energy into the gas and terminate the discharge before discharge current concentrations (streamers) can link up into a completed arc [Savic and Kekez 1977]. Reducing localised electric field concentrations by smoothly profiling the discharge electrodes delays the appearance of streamers. Some lasers use only these first two techniques [Jetter and Gurs 1976].

Photo-ionisation of the laser gas immediately before voltage is applied to the contoured discharge electrodes provides a large initial electron density between the electrodes. The discharge is rapidly established and depletes the capacitive energy store before streamers can grow significantly. Preionising spark arrays are mounted inside mesh electrodes [Richardson et al. 1973] or near solid electrodes [Richardson et al. 1972] to flood the laser mixture with hard ultraviolet.

We have constructed two ultraviolet preionised lasers with profiled solid electrodes. The mechanical design of both was identical but the second, described here, incorporated many improvements principally in the disposition of the main discharge circuit. This laser, commissioned in January 1978, is capable of twice the energy output and has a far wider wavelength range than the first laser which commenced operating in June 1976.

## 2. LASER CONSTRUCTION

The Perspex box containing the electrodes was mounted above an oil tank holding the discharge capacitors, charging resistors and the sparkgaps (Figure 1). The laser mirrors were mounted on steel posts bolted to the one-metre thick, reinforced concrete floor of a ground-floor laboratory.

The main storage capacitors ( $C_s$ ) occupied the centre of the tank and were mounted above a triggered sparkgap. A close-fitting earth return sheath surrounded the  $C_s$  and continued up past each side of the Perspex box where it connected to the upper profiled discharge electrode. The earth sheet was 27 cm wide for low inductance (see Section 3.2).

## 2.1 Laser Box

The laser box was constructed of sheet Perspex with O-ring sealed side panels for easy access to all interior components. The interior dimensions of the box were 14 cm (height) 17 cm (width) and 73 cm (length) with a total volume of 17  $\ell$ . Subtracting the volume of the Rogowski electrodes (3  $\ell$ ) gave a 14  $\ell$  swept volume. Since the box leakage rate was less than 1  $\ell$  Pa s<sup>-1</sup>, changing the gas every 15 min was enough to prevent significant leak-induced oxygen contamination (see Section 5.2).

An aperture at each end of the box limited the laser beam diameter to 38 mm. The inside surfaces of these apertures were threaded to prevent undesirable reflections. The box was strong enough to stand complete evacuation.

## 2.2 Rogowski Electrodes

The main electrodes had a Rogowski  $\pi/2$  profile [Chang 1973] designed for operation at a spacing of 20 mm although they were usually operated at a 30 mm spacing.

The electrodes were milled from A2011-T6 aluminium alloy bar stock with the Rogowski profile smoothly blended into the central area where the Rogowski profile deviated by 0.1 mm from flat (Figure 2). At the electrode ends the profile was simply rotated about the electrode centre line. No special tendency was noted for inter-electrode arcs to occur at the doubly curved electrode ends. The overall flatness of the finished electrodes was better than 0.1 mm.

The electrode surfaces were finished by lapping them with P1200 grade abrasive paper to reduce reflections.

A Perspex carrier frame supported the electrodes at the correct spacing inside the box and decoupled the box flexure which occurs as the internal pressure is varied.

### 2.3 Preionisation Arrays

Ultraviolet preionisation of the gas mix was provided by linear arrays of sparks (flash rods) disposed down each side of the box level with the mid-plane of the inter-electrode gap. This placed the spark arrays 7.5 cm from the centre of the main discharge and 4.5 cm from the nearest line on the Rogowski electrodes. Each flash rod consisted of a borosilicate glass tube (33 cm long 8 mm dia.) with a bore of 2 mm. A close-fitting earthing rod filled the tube and stainless steel spark electrodes were clipped along the outside of the tube. Squares of stainless steel, 0.2 mm thick were bent along one diagonal and slid on to the tube, spaced at 2 mm between electrode tips. The squares each had a capacitance of about 0.4 pF to the central earthing rod. Seventeen sparkgaps were mounted on each rod.

Four rods were used, the high voltage being applied near the ends of the box and the earth being connected at the centre of each of the two sides.

### 2.4 Brewster Window Holder

It was necessary to separate the sometimes doped discharge module from the diffraction grating to prevent contamination of the grating surface. A sodium chloride window mounted at the Brewster angle ( $56.5^\circ$ ) prevented losses through surface reflection. The NaCl window was sealed onto the flat surface with silicon grease. A recess around the edge of the aperture received the excess grease and prevented it from being vaporised by the laser beam.

A square aperture (Figure 3), instead of the more usual circular aperture, maximised the useful area of the beam when using a 75 mm diameter sodium chloride window. The projected height of the aperture matches the 30 mm spacing of the Rogowski electrodes. Stray internal reflections were prevented by sandblasting the inside surfaces of the Brewster window holder.

## 3. DISCHARGE CIRCUITS

Both the preionisers and main discharge were supplied from capacitive energy stores mounted, along with ballast resistor chains and triggered sparkgaps, in a tank full of transformer oil directly under the discharge module (see Section 2). Oil immersion of the d.c. charged sections allowed a

compact assembly to be constructed without corona problems in a tank 80 cm x 28 cm x 50 cm deep.

Special oil resistant ballast resistors were needed, since the surface coating of less expensive wire-wound resistors was found to slough off after a few weeks' immersion in the transformer oil.

In normal operation the preioniser arrays had to fire before the main discharge circuit, but not more than about 5  $\mu$ s before the main circuit when a substantial proportion of the transient photo-ionisation would have died away (see Section 5.3). The laser was normally operated with a 2.5  $\mu$ s inter-pulse delay.

### 3.1 Preionisation Circuit

Carbon dioxide is opaque throughout the vacuum ultraviolet except for a narrow region about 120 nm (10.3 eV) and for wavelengths longer than 170 nm (<7.3 eV) [McKen and Seguin 1976]. Since the ionisation potentials of CO<sub>2</sub>, N<sub>2</sub> and He are 14.4, 15.5 and 24.5 eV respectively, it seems two photons would be needed to ionise any of them. It has been demonstrated that impurities present in the helium are responsible for virtually all the observed photoionisation, and that low inductance spark discharges produce more photoionisation [McKen and Seguin 1976; Norris and Smith 1977b]. A type of charge transfer circuitry was used which is commonly employed to decouple switch inductance from the laser discharge loop in nitrogen lasers [Targ 1972] (Figure 4). When the sparkgap was triggered, charge was transferred from the storage capacitor (C<sub>s</sub>) to the peaking capacitor (C<sub>p</sub>) via an RG-213 coaxial cable. The voltage on the peaking capacitor rose to the prompt breakdown threshold voltage of the flash rod, and C<sub>p</sub> rapidly discharged through the low inductance flash rod.

Because every electrode on the flash rod was capacitively earthed, the full pulsed voltage was initially applied only to the first sparkgap. After the first gap had broken down the full voltage was applied to the second gap and so on until all 17 sparkgaps had broken down in quick succession. The capacitive earthing greatly reduced the voltage needed to break over the string of 17 sparkgaps [Richardson et al. 1973]. A trigger delay of 50 ns was typical.

Each of the four flash rods was individually supplied from a 2.4 nF peaking capacitor pack mounted on the side of the discharge box. Each peaking capacitor pack was pulse-charged from a flexibly mounted pack of 8 x 920 pF 40 kV working doorknob capacitors. A single triggered sparkgap switched all four packs.

The current through the flash rods was measured using a Rogowski coil and was a heavily damped sinusoid with a 300 ns period. When the flash rod's visible sidelight was examined (Figure 5) peaks of light emission were seen at about a 150 ns spacing as would be expected. The light emission was optimised by varying  $C_p$  and was at a maximum for  $C_p = 2.4$  nF or about  $C_s/3$  which is usually the case with charge transfer circuits.

### 3.2 Main Discharge Circuit

Very low inductance discharge circuits can be constructed using Blumleins [Brink and Hasson 1978] or LC generators [Chang and Wood 1972], but these circuits are usually very limited in energy storage and depend, for their efficiency, on achieving a 100 per cent voltage reversal in one of their two capacitor packs. The typical capacitor life-shortening factor is twenty to a hundredfold for a 100 per cent voltage reversal.

A simple discharge circuit (Figure 6) was used in which both Rogowski electrodes were usually grounded, and the triggered sparkgap had one grounded electrode. Two 50 nF capacitors were mounted in the oil tank (Figure 7), symmetrically beneath the discharge module. Each capacitor had a self-inductance of 33 nH which was negligible compared to the overall inductance of 150 nH. The section below the discharge module, which was connected to the lower Rogowski electrode by a 25 cm wide flexible sheet conductor, had an inductance of 70 nH. It would be unrewarding to try to reduce the 80 nH inductance of the top half without reducing the size of the Perspex box.

Rogowski coil measurements showed that the 5000A main discharge current pulse had a 500 ns full width at half maximum height and no reversal occurred.

The quoted life expectancy of the Condenser Products EMB 50MPXL capacitor was only  $3 \times 10^5$  shots, but by operating the capacitors at least 10 kV below their 50 kV rated working voltage and avoiding arc discharges, we have already

had over three times that life out of them.

### 3.3 Triggered Sparkgaps

A common sparkgap design was used for both the discharge circuits. The design incorporated several features to improve the trigger timing accuracy and increase the lifetime.

Both the cathode and anode surfaces (Figure 8) were of tungsten-copper alloy as was the large diameter trigger disc. The polarities indicated were most important. Asymmetric sparkgaps provided the minimum formative time lag when the trigger spark was in the anode and illuminated the cathode surface. The trigger pulse was positive, maximising the electrical stress on the main gap.

The cathode was Rogowski  $2\pi/3$  profiled [Chang 1973] to reduce the incidence of field-concentration induced, spontaneous breakdown of the anode-cathode gap. The 8 mm main gap did not spontaneously break down when 26 kV was applied and the gap was unpressurised.

A ceramic (pyrophyllite) insulator positioned in the trigger gap annulus forced the trigger spark to track over the front surface of the insulator, where its ultraviolet emission illuminated the main gap cathode. The trigger threshold voltage of the main gap was only 9 kV at 200 kPa gauge pressure of nitrogen. In the preioniser circuit which usually operated at 26 kV, with a stored energy of 10 J, wear on the ceramic insulator was negligible but, in the low inductance main discharge circuit (60 J, 35 kV), the trigger components needed replacement after every 250 000 shots.

The wear was evidently caused by the main discharge current which followed the trigger spark path across the ceramic surface. The trigger disc was deliberately thinned so that the trigger spark would move to a fresh position before evaporating too deep a groove in the insulator surface. Experiments to find harder wearing ceramics are continuing but at present unfired pyrophyllite seem to last much longer than fired pyrophyllite.

If the ceramic insulator was not fitted the main gap would sometimes fail to trigger even though the trigger gap fired every time.

The performance of the sparkgaps was studied as a function of voltage, gas pressure and trigger source impedance. The normal operating conditions for the gaps were 140 kPa flowing nitrogen pressure and a 35 kV applied voltage. Figure 9 shows that an acceptable trigger delay ( $<200$  ns) was obtained at 25 kV even when the gap was pressurised at 235 kPa and that, although any of the conditions chosen provided a suitable trigger delay at 35 kV, the triggering was better when the sparkgap was isolated from the trigger source by a few kilohms.

These results, obtained after 250 000 shots had been fired by the gap, contrast with the performance of a sparkgap without a trigger insulator bush which would behave similarly for the first few tens of thousands of shots and then deteriorate rapidly as the edge wore off the trigger electrode.

### 3.4 Trigger Generation

The pair of trigger pulses required to drive the laser were produced by an AAEC type 534 twin laser trigger unit [AAEC 1974] in which a pair of English Electric type CV8503 thyratrons, driven by prompt and delayed pulse generators, discharged 4 nF 9 kV doorknob capacitors through 1:5 pulse transformers. The trigger rate was adjustable in 1 Hz steps from 1-50 Hz and the interpulse delay could be continuously adjusted from 0.1-22  $\mu$ s in three ranges, a feature which we have found very useful in synchronising two TE lasers. The high trigger rate feature was of little use with this laser since the maximum rate of a couple of hertz was determined by gas heating problems.

The trigger transformers used strip-wound supermumetal cores (0.8 cm<sup>2</sup> area, 10 cm path length) each of 25  $\mu$ m thick strip. A four-turn helical primary and a twenty-turn helical secondary winding were used.

The output pulse into 4.7 k $\Omega$  reached 40 kV, and had a width of 75 ns and a risetime of 25 ns which was mainly determined by interwinding and stray capacitive loading.

#### 4. THE OPTICAL CAVITY

Two distinct optical cavities were used. When the maximum output energy was required regardless of wavelength, vacuum sealing mirrors were used at each end of the laser box. Mirrors (50 mm dia.) at each end allowed maximum use to be made of the gain medium. The mirror at one end was plane and of gold-coated stainless steel, the output germanium mirror was coated for 70 per cent reflection and had surfaces 20 m in radius, concave to the inside, convex to the outside. Use of a curved totally reflecting mirror might be more usual together with a plane output mirror which would eliminate lens effects in the output mirror. In this case, there was no choice but to operate the laser with a wavelength-selective plane grating and so a curved output mirror was mandatory.

It is well known that many different transverse standing wave flux distributions (modes) may be obtained from a laser resonator and that optical cavities with a low Fresnel number [McCumber 1965; Fox and Li Tingye 1961] favour low order transverse modes where the flux density is greatest on the axis of the cavity. Such modes experience lower diffraction losses in long, and thin, low Fresnel-number optical cavities. 'Gaussian' profile beams could be obtained from this laser by restricting the aperture of the cavity but only at the expense of energy (Figure 11) (Fresnel number 2).

For our application a uniform flux distribution is more desirable and can be obtained by operating the laser at maximum aperture with long radius-of-curvature mirrors. The laser was usually operated with a cavity radius of 15 mm as determined by the Brewster window and a mirror spacing of 1.7 m. The Fresnel number was at least 13 and many transverse modes oscillated.

The diffraction grating was gold-coated stainless steel with 150 grooves/mm and was blazed for 10.6  $\mu\text{m}$  operation. When operated at the Littrow angle ( $52.58^\circ$ ) it had projected dimensions of 36 x 36 mm and provided an angular dispersion of 8.1 nm/mrad, more than enough to separate fully all  $\text{CO}_2$  rotational lines [The Chemical Rubber Co. 1971]. The damage threshold of the grating was quoted by the manufacturer at 70  $\text{MW cm}^{-2}$  (later 2.1  $\text{J cm}^{-2}$ ) (see Section 6).

#### 4.1 Output Pulse Shape

With close-coupled vacuum sealing mirrors (70 per cent reflecting 10 m radius of curvature versus a plane total reflector) and with the optimum gas mix (Section 5.1) the laser produced a 6 J output pulse on the 10.59  $\mu\text{m}$  P20 vibrational-rotational transition. The input energy was 63 J from 0.1 nF, and the output energy was measured with a volume absorbing calorimeter.

The whole output beam was attenuated by calcium fluoride flats and focussed into a photon drag detector. The output pulse had a partially mode-locked spike 100 ns wide, followed by a 2  $\mu\text{s}$  tail containing about one half of the total pulse energy. It is, of course, well known that the spike and the tail have quite different transverse energy density distributions across a TE laser output beam [Decker et al. 1973], and that sampling a TE laser pulse using a small aperture gives an optimistic estimate of the spike-to-tail ratio.

When a Brewster window and grating were used in the optical cavity the higher overall losses reduced the relative spike height.

#### 4.2 Beam Characteristics and Wavelength Range

For line-selected operation with an intracavity diffraction grating and a Brewster window, the range of available output wavelengths depended on the quality of the optics and the available laser gain. Table 1 shows the pulse energies available on various high and low gain vibrational-rotational lines when the laser was set up for a wide wavelength range, not high power. Note that 4.5 J was available on the 944  $\text{cm}^{-1}$  P20 at 30 kV using mirrors and no Brewster window.

With the intracavity Brewster window installed, the output beam was 26 mm wide by 22 mm high near the output mirror and had a horizontal divergence of 2.5 mrad whilst the vertical divergence was 1.6 mrad demonstrating the vertical wavelength dispersion of the grating.

With mirrors and no Brewster, the output beam had a 7.5  $\text{cm}^2$  area in the near field.

#### 4.3 Far Field Flux Density

Using an alternative solid aluminium diffraction grating in a vacuum tight mount, the laser would be operated without a Brewster window and with an adjustable aperture as shown in Figure 10.

A 16 point scanned pyroelectric detector mounted at the focal point of a 20 m radius-of-curvature mirror produced the scans of Figure 11. In each case five successive 1 Hz shots are presented. It is clear that careful selection of output mirror transmittance can improve the uniformity of the output beam on low gain lines such as the P48, and that very uniform output fluxes can be obtained by careful adjustment of the optical cavity.

#### 4.4 Inductance and Beam Uniformity

While the laser was being assembled, the sparkgap and Rogowski electrode gap were shorted and the total discharge circuit inductance was measured as 150 nH by grid-dip meter resonance with the 0.1  $\mu\text{F}$  energy storage capacitor. Later the inductance was estimated by preventing the preionisation from functioning. The main discharge then arced with a ring period of 850 ns which corresponded to a total circuit inductance of 180 nH. This included the inductance of the 30 mm long arc.

The laser was operated with mirrors and an undoped gas mixture at  $140 \text{ J } \mu\text{s}^{-1}$  and produced a 6 J output pulse. The discharge circuit inductance was then raised by stages until streamers were apparent in the discharge at 620 nH. As the inductance was raised still further the streamers grew in length until they almost bridged the 30 mm gap at an inductance of 1.3  $\mu\text{H}$ .

Although the average output energy had dropped by less than 5 per cent over the whole inductance range, the streamers severely disturbed the output beam uniformity and appeared in the near-field beam cross section as bright-edged silhouettes.

The upper edge of the far-field beam cross section was examined using the scanned pyroelectric detector array. When the inductance was 150 nH the shot-to-shot reproducibility of the beam edge was  $\pm 5$  per cent; with the inductance raised to 1.3  $\mu\text{H}$ , shots with 60 per cent less edge energy were common.

Obviously, constancy of integrated pulse energy was no indicator of laser beam quality.

The effect of circuit inductance was again studied, two months after the organic dopant trimethylamine had been briefly used in the laser. The laser was tuned to the low gain P48 line and no change in output energy was observed as the inductance was raised to 920 nH. A few thin and scattered streamers were visible in the discharge but they produced no visible silhouettes in the output beam. The lack of severe streamer disturbances was attributed to residual dopant which has been shown [Andrews et al. 1978] to maintain TE discharge uniformity at high energy loadings. The beam uniformity could not be studied since damage to the grating had made the output beam rather spotty.

## 5. GAS HANDLING

Helium, nitrogen and carbon dioxide were regulated to 200 kPa and fed through flowmeters and needle valves direct to the discharge module. The gas was pumped out of the module through an adjustable choke which controlled the operating pressure in the module. Minor gas additives such as hydrogen, carbon monoxide and trimethylamine were sometimes used. The discharge module and manifold had a leak rate of less than  $1 \mu\text{Pa s}^{-1}$ .

### 5.1 Mixture Optimisation

The gas mix should contain the highest possible partial pressure of carbon dioxide in order to maximise the energy in the gain switched spike. Carbon dioxide molecules are not efficiently ionised by low energy electrons, and a higher electric field is needed to produce a glow discharge in  $\text{CO}_2$  rich  $\text{CO}_2\text{-N}_2$  mixtures [Nighan and Bennett 1969].

The usable proportion of carbon dioxide in our laser mix was found to depend strongly on the efficiency of the ultraviolet preionisation and was limited to less than 30 per cent by the complete failure of a discharge to occur at higher  $\text{CO}_2$  partial pressures. We found 13 per cent  $\text{CO}_2$  to be optimum for energy extraction and beam uniformity at 1 Hz operation with an undoped gas mixture.

Some CO<sub>2</sub> TE lasers will operate without any nitrogen in the gas mix (e.g. e-beam lasers) but ultraviolet preionised lasers depend on the nitrogen for virtually all the useful ultraviolet light emission from the flashrod sparks [McKen and Seguin 1976]. Nitrogen has a high cross section for electron impact ionisation [Nighan and Bennett 1969] and the excited gas couples resonantly [Denes and Weaver 1973] with the carbon dioxide to supply energy rapidly and efficiently to the carbon dioxide. The nitrogen supplies some of the energy for the gain-switched spike and all of the energy to the microseconds-long tail of the output pulse; usually 20 per cent nitrogen was used.

Helium was added to the gas mixture to raise the total pressure, to collision broaden the carbon dioxide gain profile [Denes and Weaver 1973], to enhance heat removal from the mixture and to supply the trace organic impurities needed for efficient ultraviolet preionisation [McKen and Seguin 1976] of undoped gas mixtures. Sharper gain-switched spikes are available from collision broadened gas mixtures. Helium consumption could be reduced by operating the laser at reduced pressure (e.g. simply reduce the helium flow) or by deliberately doping the gas mix with trimethylamine [Vedenov et al. 1976]. The comparative output energies were 6 J with an undoped 66 per cent helium mixture and 0.5 J with an undoped helium free mixture.

The optimum operating conditions were a pressure of 90 kPa at a flow of  $45 \times 10^3 \text{ g Pa s}^{-1}$  of 10:2:3 (He, CO<sub>2</sub>, N<sub>2</sub>) undoped gas mixture. The gas in the discharge module changed every 30 s but the laser performance would be improved if the flowrate could be greatly increased. Tests showed that small streamers present in the discharge at 1 Hz entirely disappeared when the laser was operated at 0.2 Hz, a clear indication that discharge-induced heating of the laser gas was a problem.

## 5.2 Gas Impurities

Water vapour and oxygen both have a high molar absorptivity in the vacuum ultraviolet (water  $200 \text{ cm}^{-1}$  at 120 nm) [Watanabe and Zeilkoff 1953], and reduce the penetration of the preionising light. In addition, oxygen has a high electron attachment coefficient [Norris and Smith 1977a] and consumes photo-electrons, thus interfering with the discharge growth.

If the water content of the feed gases is kept below 100 ppm, the attenuation of 120 nm light is less than 20 per cent over a 10 cm path length. All commercial pressurised gases have a water content of less than 100 ppm if the cylinders are discarded after 80 per cent of their contents are used. However it has been found necessary to keep the gas system filled with laser mix at all times to prevent pickup of atmospheric water. In a leak-tight system, oxygen impurities are supplied with the feed gas or generated in the discharge volume by decomposition of  $\text{CO}_2$ . 'Industrial Dry' grade nitrogen has too high an oxygen content ( $< 2000$  ppm) and 'High Purity Oxygen Free' nitrogen (specified as typically  $< 25$  ppm oxygen) was regularly used in undoped gas mixtures. Unfortunately the oxygen content of the 'High Purity Oxygen Free' nitrogen fluctuated from cylinder to cylinder and sometimes was measured by mass spectrometry as  $>500$  ppm. Arcing which started when a fresh nitrogen cylinder was connected was easily recognised as being caused by excessive oxygen and the offending cylinders emptied and discarded.

No such problem was ever noticed with the carbon dioxide or helium supplies. The erratic variation in the oxygen content of the available nitrogen supplies is a good reason to add organic dopants to the gas mix to ensure consistent laser performance. When a few ppm of trimethylamine (see Section 5.3) was added to the laser gas mixture the preionisation was so good that either grade of nitrogen was satisfactory.

### 5.3 Gas Additives

Hydrogen [Norris and Smith 1977a] and carbon monoxide [Gibson et al. 1978] have been reported to prevent oxygen buildup in  $\text{CO}_2$  TE lasers.

A few per cent of hydrogen was added to the gas mix and produced no significant improvement, possibly because the hydrogen provokes  $\text{CO}_2$  decomposition and water formation; hydrogen is no longer used in the gas mix.

Carbon monoxide addition at up to 10 per cent of the total flowrate caused no significant change in the laser performance.

Xylene, n-n dimethylaniline [Grosjean and Bletzinger 1977] and various amines [Seguin et al. 1976] have low photoionisation energies and are often added to laser gas mixtures to enhance the ultraviolet preionisation. The addition of a few hundred ppm of trimethylamine to the laser mix made the

discharge very stable and quite insensitive to changes in the ratios of the helium, carbon dioxide and nitrogen. The organic dopant was very persistent and all measurements with undoped gas mixtures were made before any had ever been added. Persistent dopant greatly improved the uniformity of high inductance discharges (see Section 4.5).

When excessive amounts of trimethylamine were used (5000 ppm) the main discharge split into two separate glows, one down each side of the Rogowski electrodes rather than in the centre which was further from the flash rods. The glows were so far away from the optic axis that the device would not lase.

## 6. MAINTENANCE

Regular maintenance was needed to maintain the laser's performance. Every three months (250 000 shots) the anode, dielectric bush and trigger pin of the main discharge-triggered sparkgap were found to be worn and in need of replacement to restore the gap's trigger performance. The other triggered sparkgap switched one sixth of the energy and had a much lower wear rate. The trigger components of this sparkgap were replaced every six months when, in any case, the flash rods and laser box were in need of attention.

The flash rod sparks decomposed some carbon dioxide with each shot, and after six months this carbon dust coated the floor of the Perspex box to such an extent that flashovers occurred from the Rogowski electrode to the flash rods across the bottom of the box, four times the length of the shortest path.

The gap between the flash rod spark electrodes eroded from 2 mm to 3 mm over six months and conducting (10 k $\Omega$ ) tracks developed across the rod surface. Eventually surface conduction along the tracks prevented the flash rods from promptly triggering. The slide-on electrodes were rotated to a fresh area of the rod surface and closed up to a 2 mm spacing.

The carbon film covering the Rogowski electrodes was cleaned off every six months and the electrodes were lapped with P1200 grade abrasive paper to prevent troublesome parasitic reflections.

No problems occurred with the semi-transparent germanium mirrors or with the gold-coated stainless steel, totally reflecting mirrors. However, our use of 85 and, in some cases 95 per cent reflecting output mirrors raised the average intracavity laser flux to about  $3 \text{ J cm}^{-2}$ . Every three months the NaCl Brewster window had accumulated sufficient damage spots to interfere seriously with the output beam energy and uniformity, and the window was replaced. The particular problem was surface microspalling of the sintered polycrystalline NaCl which caused window translucency. More distressing perhaps were the damage spots which appeared on the surface of the diffraction grating after nine months' use. Microscopic examination of the grating surface revealed that the gold-coating was missing in spots and that the grooves had totally disappeared from the stainless steel in those areas. Although special care was always taken to keep dust off the grating surface it seemed that the intracavity laser flux exceeded the  $2 \text{ J cm}^{-2}$  and  $70 \text{ MW cm}^{-2}$  damage threshold of the grating and the grooves were removed by corrosion of the stainless steel by carbonised dust. A grating treated similarly but exposed to half the flux has so far shown no sign of damage.

## 7. CONCLUSIONS

The solid Rogowski electrode laser described above is capable of producing uniform far-field flux densities. Using low inductance discharge circuits produces a worthwhile improvement in the discharge uniformity but at the expense of more rapid sparkgap wear.

Organic doping of the laser gas mix is an easier way to achieve discharge uniformity but the decomposition products tend to coat the box and the flash rod gaps which promote conducting bridges between the flash rod electrodes.

Hot carbon dust is very corrosive to stainless steel and the presence of carbon dust in the laser box indicates that a long life should not be expected from a stainless steel diffraction grating if it is to be directly exposed to the laser gas mixture. The experience gained here with externally mounted gratings using loose dust covers demonstrates that vacuum tight covers are needed. A dust-free laboratory would be helpful; obviously the widespread practice of using graphite blocks to view the beam is quite undesirable.

The maximum desirable intracavity laser flux has been reached (or even passed) and if a wider wavelength range is needed, serious consideration would have to be given to an oscillator-amplifier configuration to lengthen the grating life.

## 8. ACKNOWLEDGEMENT

Mr J. Woodhouse was responsible for the mechanical design and assembly of this laser which was built by the Instrument Workshop, Engineering Services Department.

## 9. REFERENCES

- AAEC [1974] - AAEC type 534 Twin Laser Trigger. AAEC internal report.
- Andrews, K.J., Bhatnagar, R., Dyer, P.E. and Salvetti, G. [1978] - Studies of a high performance TE CO<sub>2</sub> laser using additives. Opt. Comm., 26 (2) 228-32.
- Beaulieu, A.J. [1970] - Transversely excited atmospheric pressure CO<sub>2</sub> lasers. Appl. Phys. Lett. 16 (12) 504-5.
- Brink, D.J. and Hasson, V.L. [1978] - High-power photo preionisation-stabilised carbon dioxide waveguide lasers operating at gas pressures up to 13 atm. J. Appl. Phys., 49 (4) 2250-53.
- Chang, T.Y. [1973] - Improved uniform field electrode profiles for TEA laser and high voltage applications. Rev. Sci. Instrum., 44 (4) 405-7.
- Chang, T.Y. and Wood, O.R. [1972] - A simple self mode locked atmospheric pressure CO<sub>2</sub> laser. IEEE JQE, 8 (8) 721-3.
- Chemical Rubber Co. [1971] - Handbook of Lasers. (ed. Pressley, R.J.), pp. 329-333.

- Decker, G., Kellerer, L. and Rohr, H. [1973] - Construction, operation and properties of TEA CO<sub>2</sub> lasers. Max Planck Institute for Plasma Physics. Garching report No. IPP 1/134.
- Denes, L.J. and Weaver, L.A. [1973] - Laser gain characterisation of near-atmospheric CO<sub>2</sub>:N<sub>2</sub>:He glows in a planar electrode geometry. J. Appl. Phys., 44 (9) 4125-36.
- Fox, A.G. and Li, Tingye. [1961] - Resonant modes in a laser interferometer. Bell Sys. Tech. J., 40 (2) 453-88.
- Gibson, R.B., Javan, A. and Boyer, K. [1978] - Sealed multiatmosphere CO<sub>2</sub> TEA laser: Seed-gas compatible system using unheated oxide catalyst. Appl. Phys. Lett., 32 (11) 726-7.
- Grosjean, D.F. and Bletzinger, P. [1977] - Photoionisation and photoabsorption characteristics of laser seed compounds. IEEE JQE, 13 (11) 894-904.
- Jetter, H. and Gurs, K. [1976] - A simple 100 MW tunable CO<sub>2</sub> TEA laser volumetrically excited without using any preionisation. Opt. Eng., 15 (7) 17-19.
- McCumber, D.E. [1965] - Eigenmodes of a symmetrical cylindrical confocal laser resonator and their perturbation by output coupling apertures. Bell Sys. Tech. J., 44 (2) 333-63.
- McKen, D.C. and Seguin, H.J. [1976] - Photoionisation parameters in the carbon dioxide laser gases. IEEE JQE, 12 (8) 470-82.
- Nighan, W.L. and Bennett, J.H. [1969] - Electron energy distribution functions and vibrational excitation rates in CO<sub>2</sub> laser mixtures. Appl. Phys. Lett., 14 (8) 240-3.
- Norris, B. and Smith, A.L.S. [1977a] - Attachment loss of photoionisation electrons in TEA CO<sub>2</sub> lasers. J. Phys. D., Appl. Phys., 10 : L237-40.

- Norris, B. and Smith, A.L.S. [1977b] - Operation of sliding spark arrays for laser preionisation. J. Phys. E., 10 (5) 551-4.
- Pearson, P.R. and Lamberton, H.M. [1972] - Atmospheric pressure CO<sub>2</sub> laser giving high output energy per unit volume. IEEE JQE, 8 (2) 145-9.
- Richardson, M.C., Alcock, A.J., Leopold, K. and Burtyn, P. [1972] - A high power CO<sub>2</sub> TEA laser. Proc. Symp. High Power Molecular Lasers, Laval Univ., Quebec, Canada, 15-17 May.
- Richardson, M.C., Leopold, K. and Alcock, A.J. [1973] - Large aperture CO<sub>2</sub> laser discharges. IEEE JQE, 9 (9) 934-39.
- Savic, P. and Kekez, M.Ā. [1977] - A study of breakdown delay in electrically pumped gas lasers. Can. J. Phys., 55 : 325-36.
- Seguin, H.J.J., Mcken, D. and Tulip, J. [1976] - Source emission and photoelectron production in a seeded CO<sub>2</sub> laser mixture. Appl. Phys. Lett., 29 (2) 110-2.
- Targ, R. [1972] - Pulse nitrogen laser at high repetition rate. IEEE JQE, 8 (8) 726-8.
- Vedenov, A.A., Drobyazko, S.V., Egorov, A.A., Zhuravskii, L.G. and Turundaevskii, V.B. [1976] - Pulse periodic open cycle CO<sub>2</sub> laser with an average output power of 500 W. Sov. J. Quantum Electron, 6 (11) 1359-61.
- Watanabe, K. and Zeilkoff, M. [1953] - Absorption coefficients of water vapour in the vacuum ultraviolet. J. Opt. Soc. Amer., 43 (9) 753-5.
- Wood, O.R. [1974] - High pressure molecular lasers. Proc. IEEE 62 (3) 355-97.
- Yu-Li Pan, Bernhardt, A.F. and Simpson, J.R. [1972] - Construction and operation of a double-discharge TEA CO<sub>2</sub> laser. Rev. Sci. Instrum., 43 (4) 662-6.



TABLE 1

WAVELENGTH RANGE		
Rotational	Line Frequency ( $\text{cm}^{-1}$ )	Energy J
P20	944.2	2.3
P4	957.8	2.0
R2		1.4
R42	988.6	2.0
R44	989.6	1.5
R46	990.6	1.0
P50	1016.7	0.5
P48	1018.9	1.0
P46	1021.0	1.5
P44	1023.2	1.8

30 kV 0.1  $\mu\text{F}$ , 85 per cent reflecting 20 m radius mirror, intracavity NaCl Brewster window with aperture 30  $\text{mm}^2$ , Jobin-Yvon grating 150 groove/mm, Scientech volume-absorbing calorimeter.



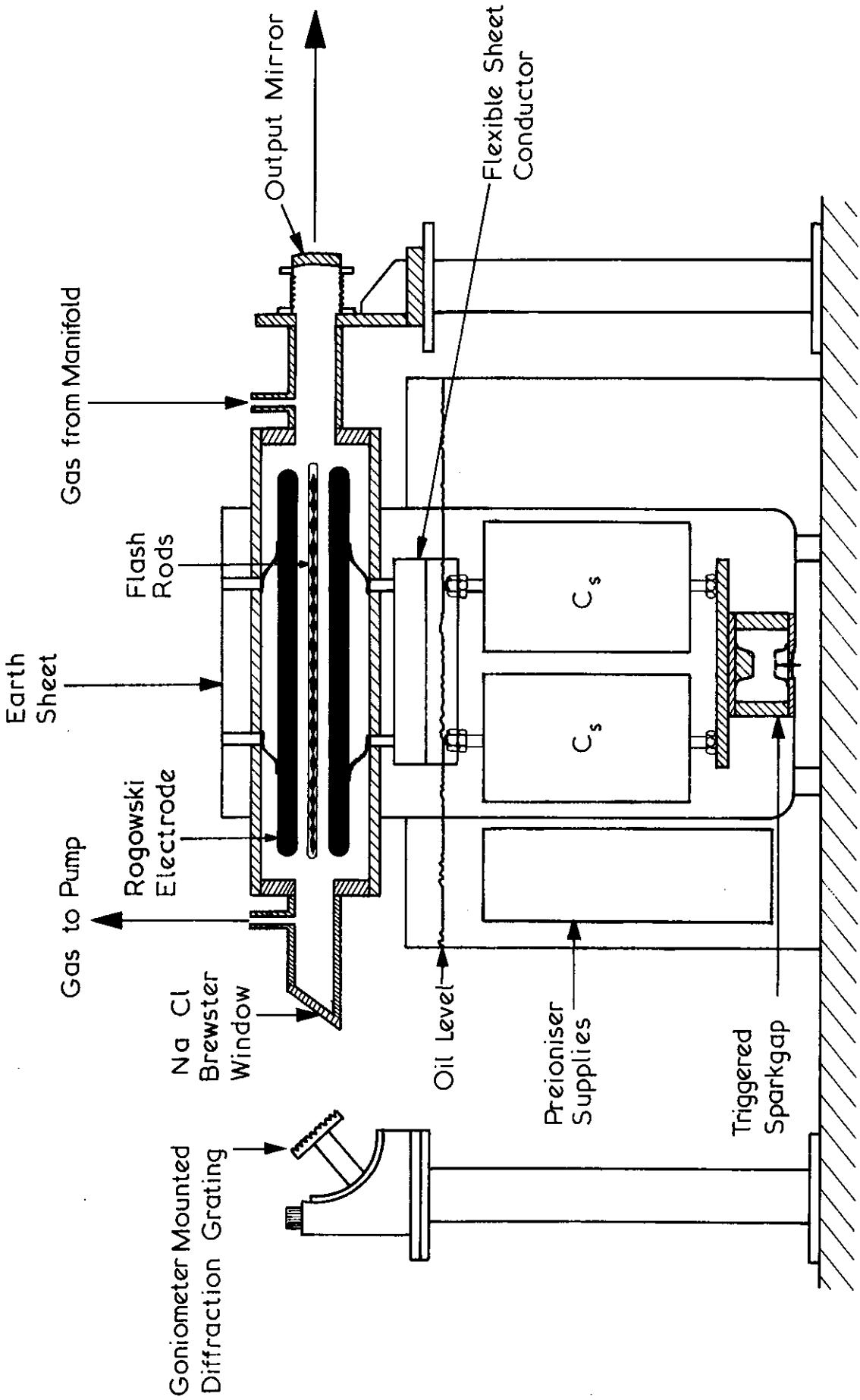
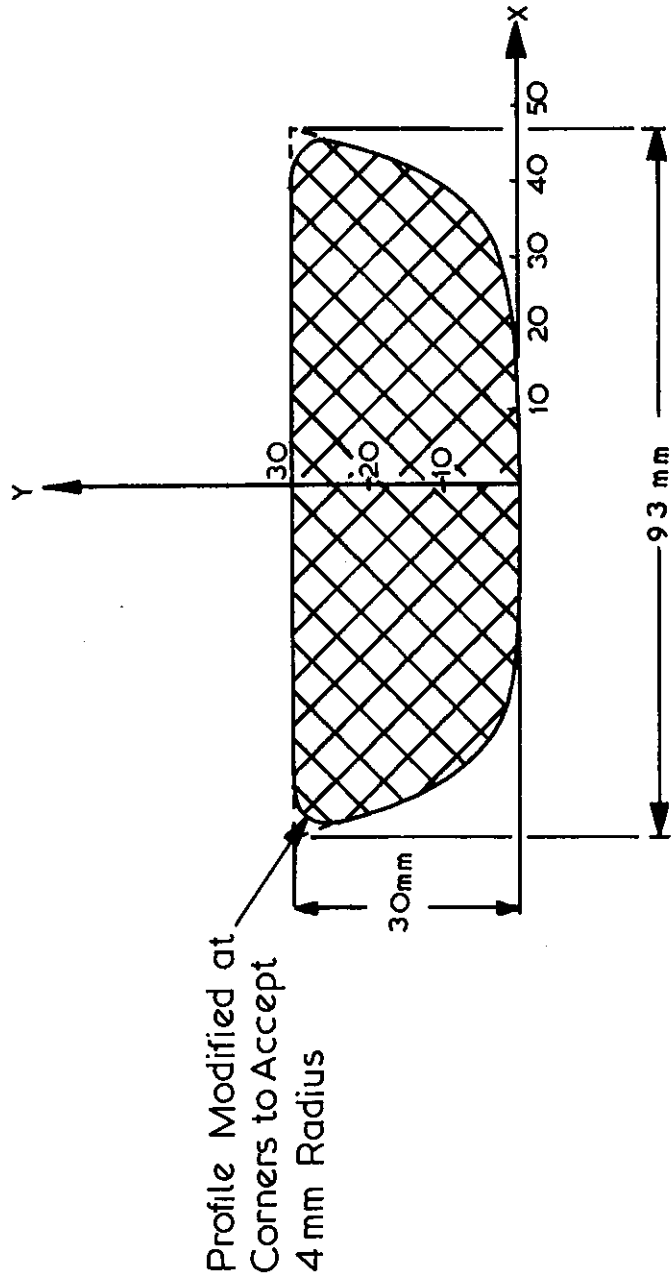


FIGURE 1. MECHANICAL LAYOUT OF LASER

X	Y	X	Y
10	0.1	40.2	11.6
17	0.3	40.5	12.0
20.2	0.5	40.6	12.3
22.4	0.7	40.8	12.6
24.65	1.0	41.0	13.0
25.8	1.2	41.1	13.3
27.2	1.4	41.2	13.6
28.4	1.8	41.4	14.0
29.05	2.0	41.6	14.3
29.65	2.2	41.9	15.0
30.2	2.4	42.1	15.6
31.2	2.8	42.4	16.3
31.6	3.0	42.7	17.0
32.2	3.3	43.0	18.0
32.8	3.6	43.2	18.5
33.5	4.0	43.4	19.0
33.9	4.3	43.6	19.7
34.3	4.6	43.8	20.3
34.9	5.0	44.0	21.0
35.3	5.3	44.2	21.6
35.6	5.6	44.4	22.3
36.0	6.0	44.6	23.0
36.4	6.3	44.8	23.8
36.6	6.6	45.0	24.5
37.0	7.0	45.2	25.3
37.3	7.3	45.3	25.7
37.5	7.6	45.4	26.1
37.9	8.0	45.5	26.5
38.1	8.3	45.6	26.9
38.3	8.6	45.7	27.3
38.6	9.0	45.8	27.8
38.8	9.3	45.9	28.3
39.0	9.6	46.0	28.7
39.3	10.0	46.1	29.1
39.5	10.3	46.2	29.6
39.7	10.6	46.3	30.1
39.9	11.0	46.4	30.6
40.0	11.3		



**FIGURE 2. ROGOWSKI  $\pi/2$  ELECTRODE PROFILE 20 mm FLAT, 20 mm SPACING**

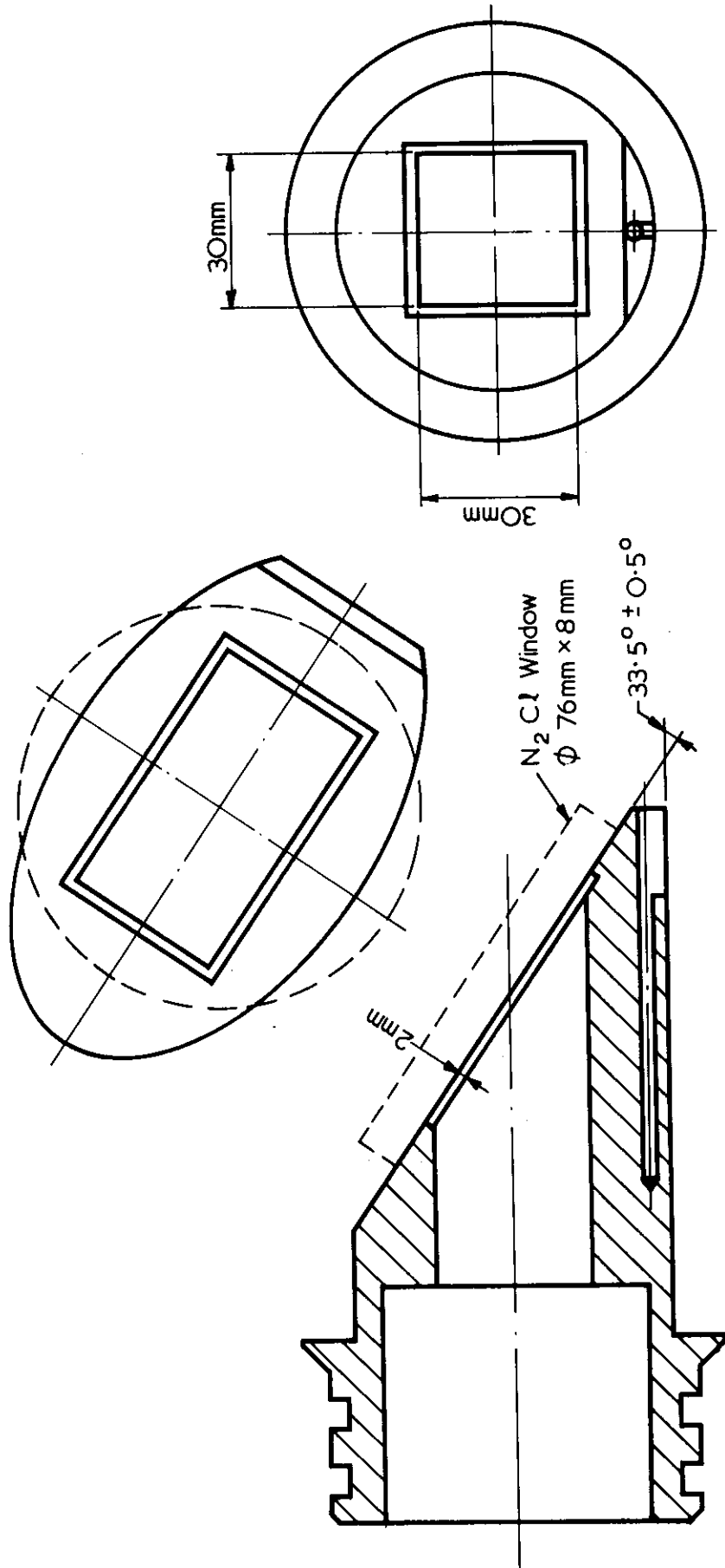
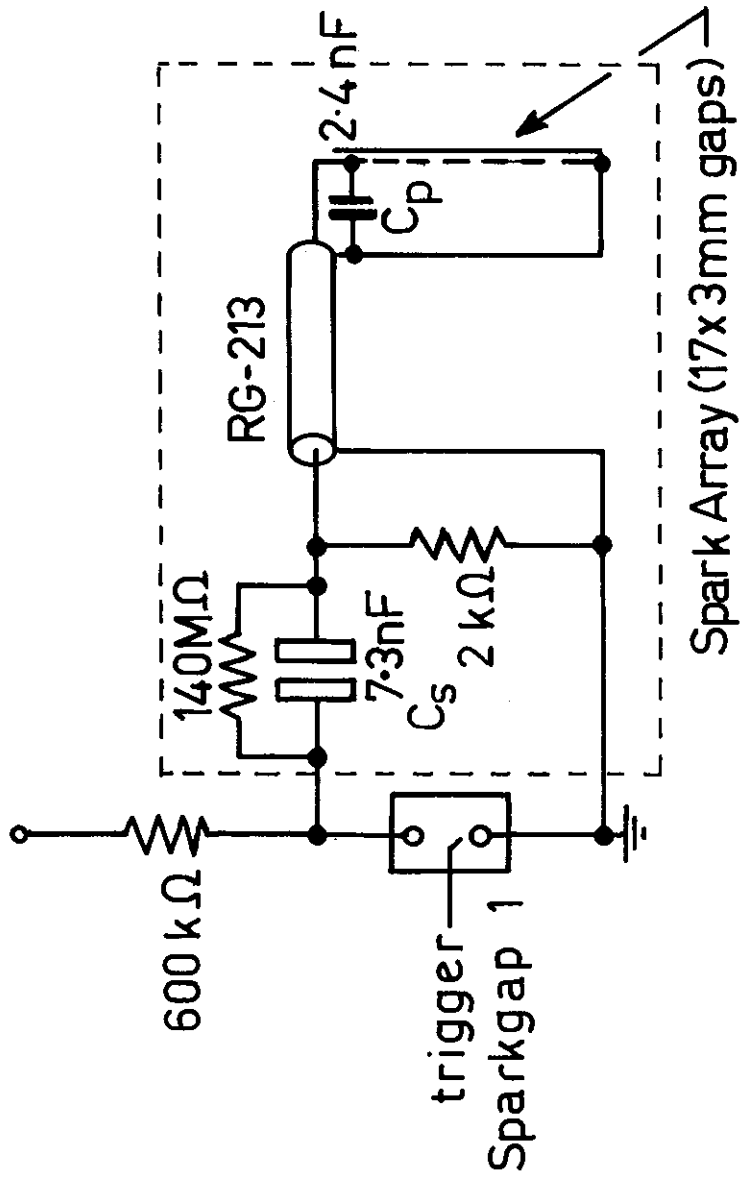


FIGURE 3. BREWSTER WINDOW HOLDER



Components inside dotted line occur four times in the circuit

FIGURE 4. UV PREIONISER CIRCUIT

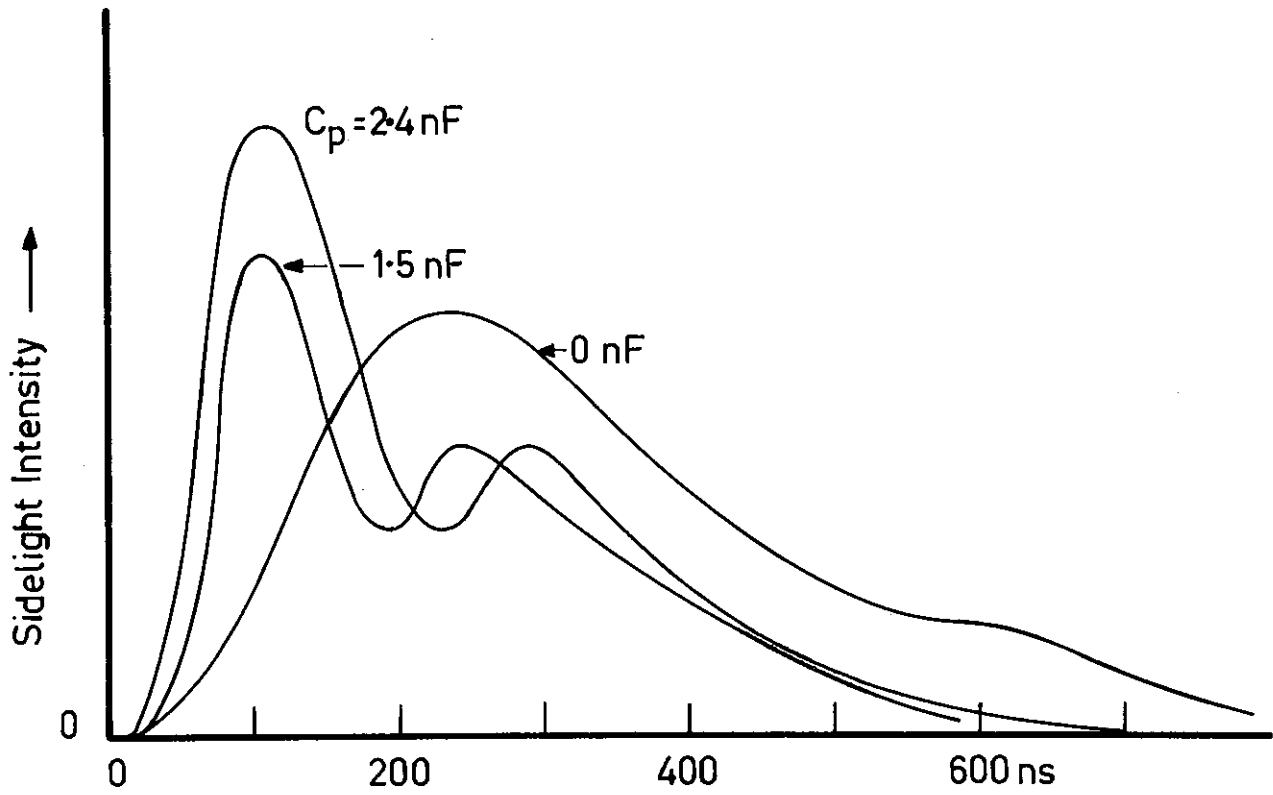


FIGURE 5. SIDELIGHT VARIATION WITH PEAKING CAPACITOR VALUE

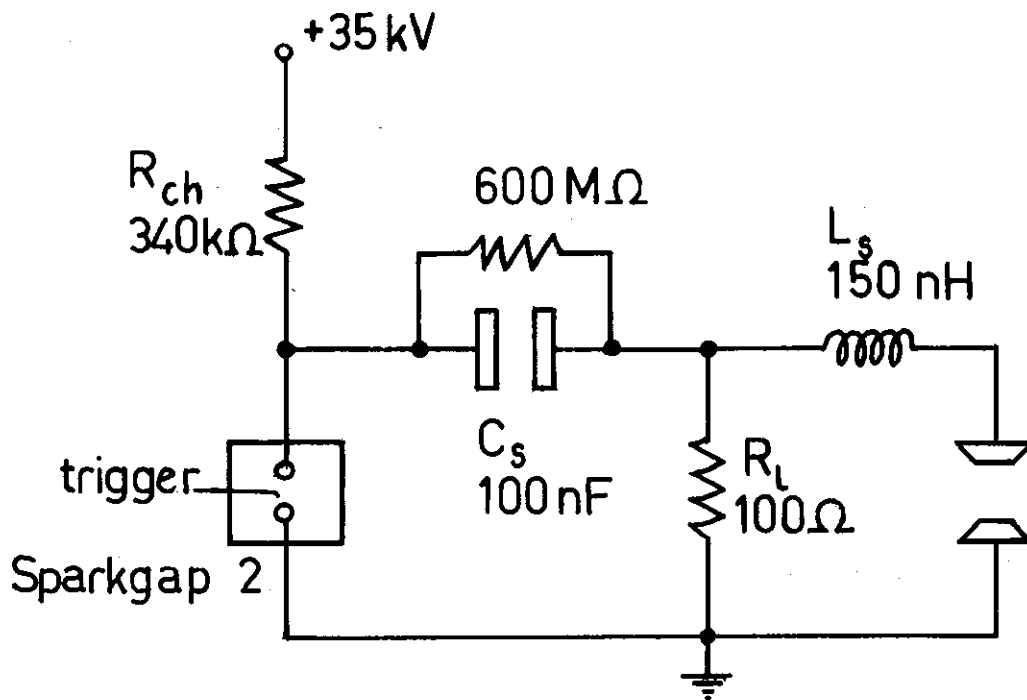


FIGURE 6. MAIN DISCHARGE CIRCUIT

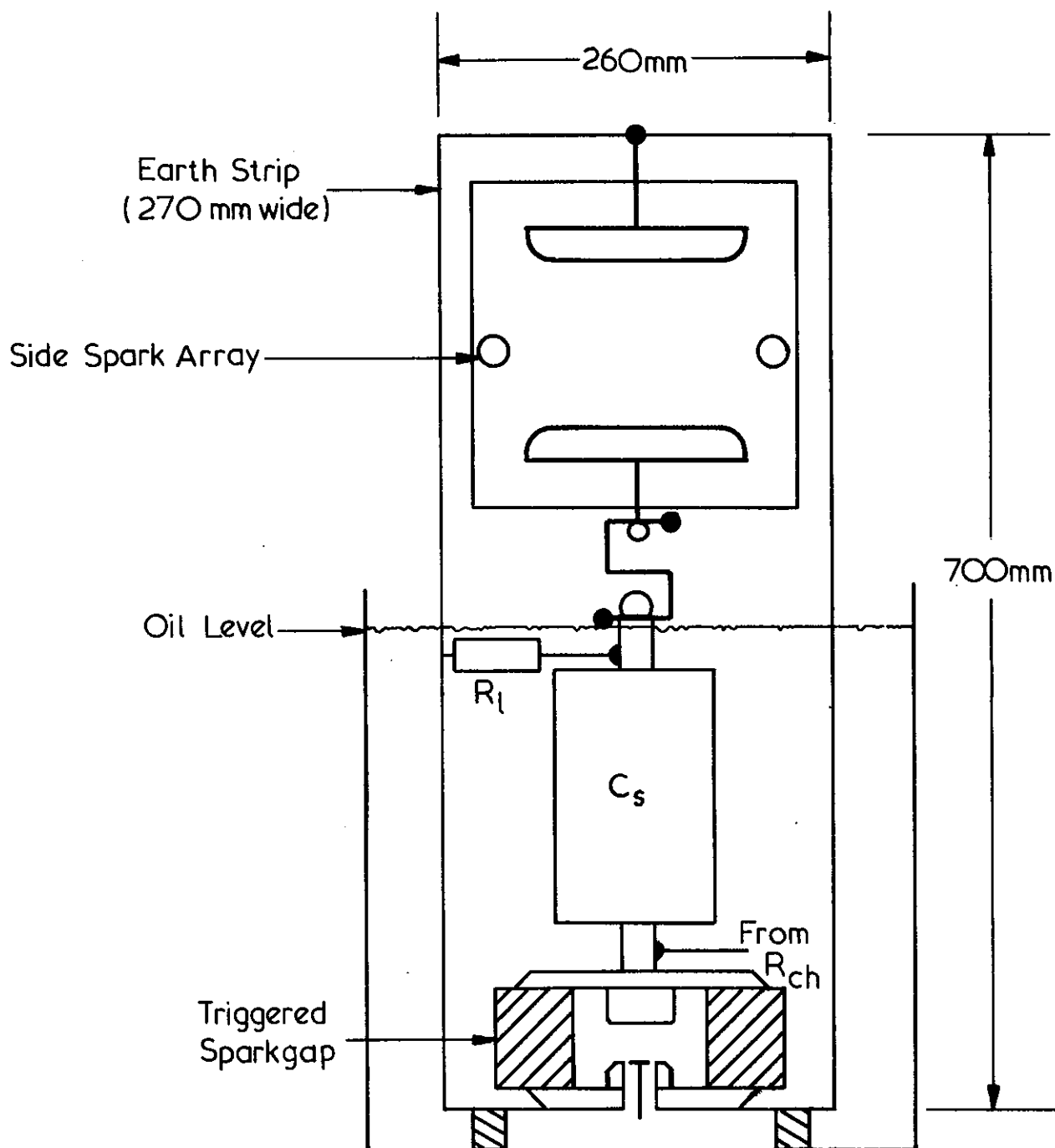


FIGURE 7. MECHANICAL LAYOUT OF MAIN DISCHARGE CIRCUIT

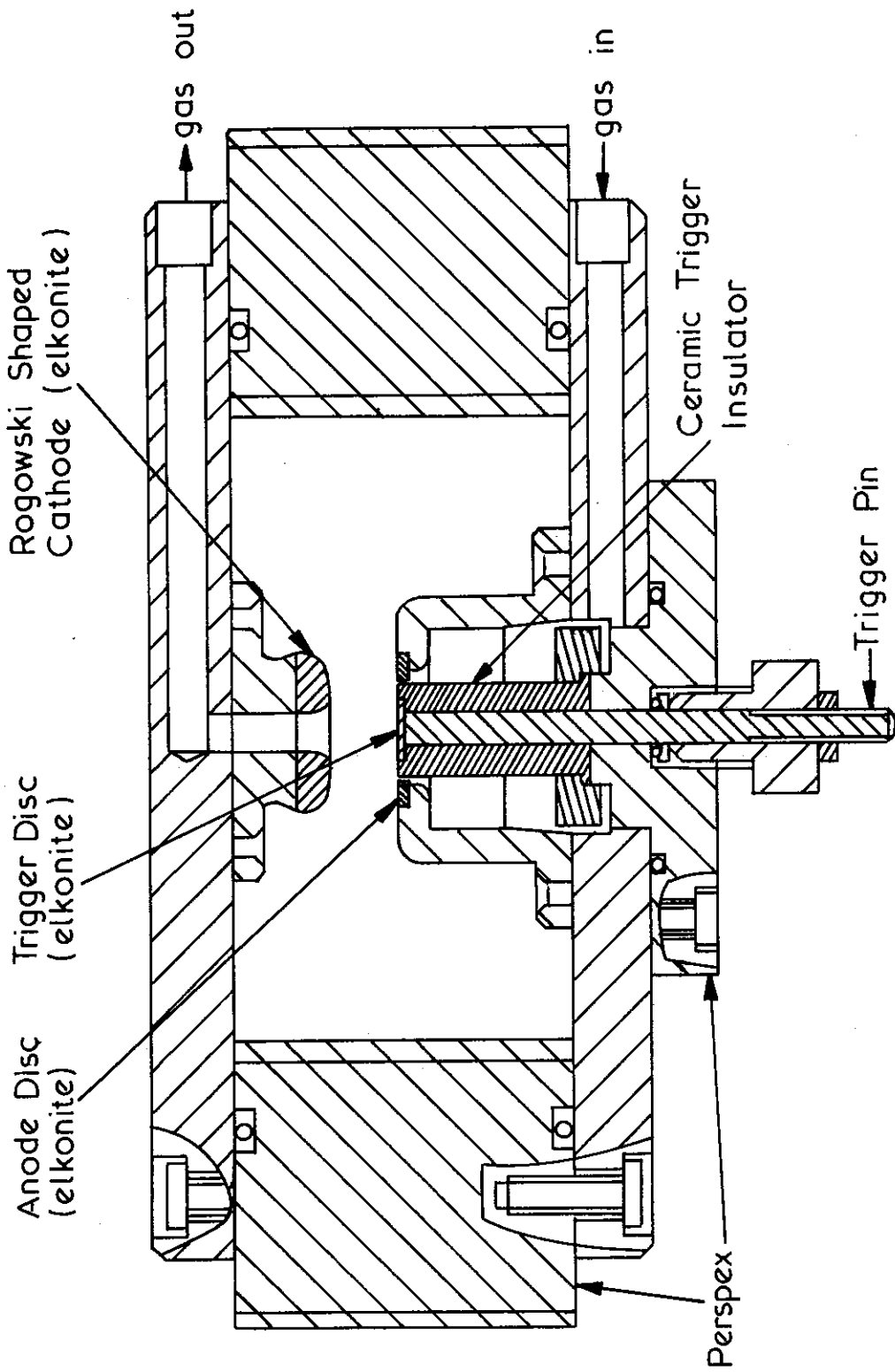


FIGURE 8. TRIGGERED SPARKGAP WITH CERAMIC TRIGGER INSULATOR

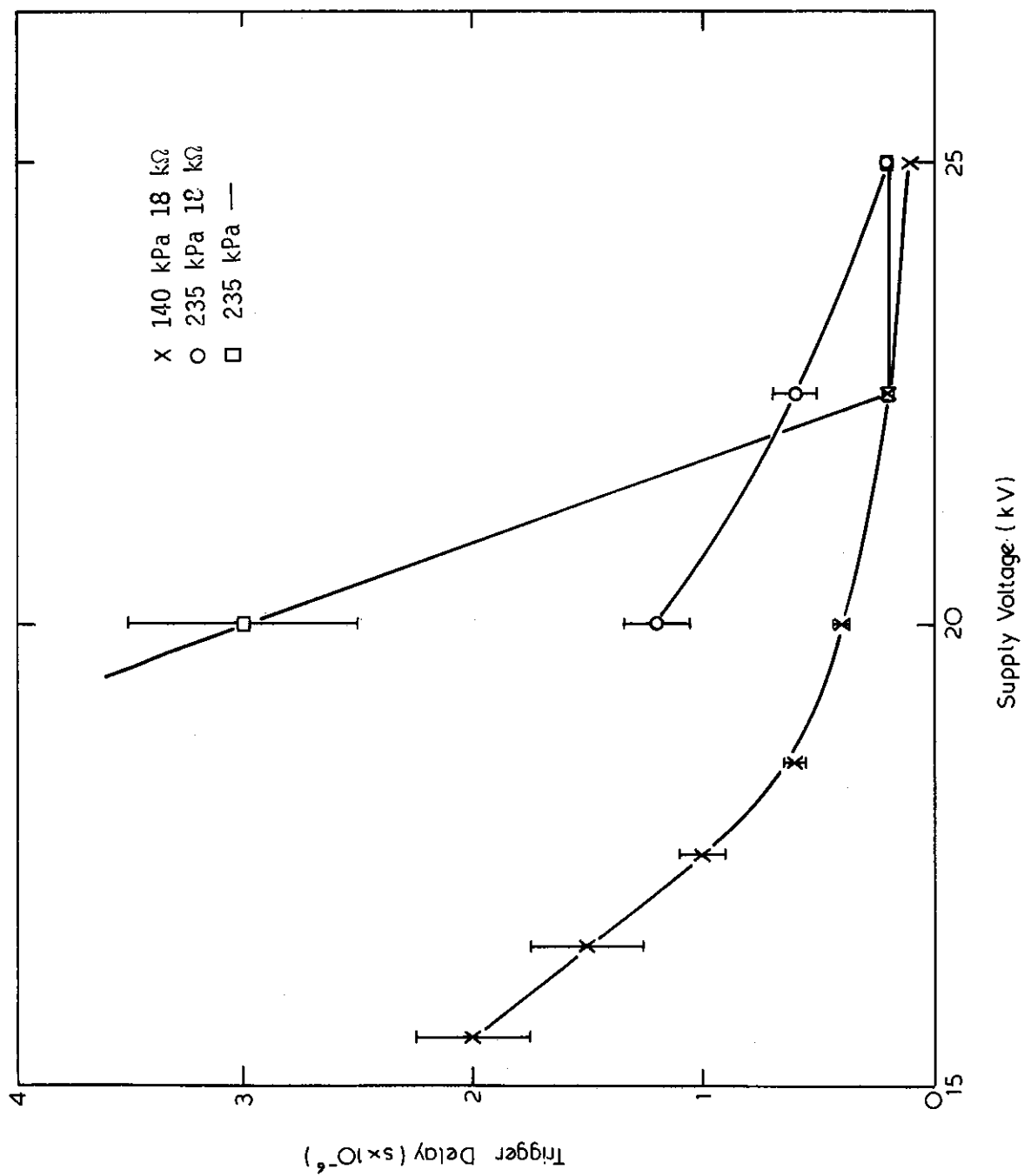


FIGURE 9. SPARKGAP TRIGGER DELAY

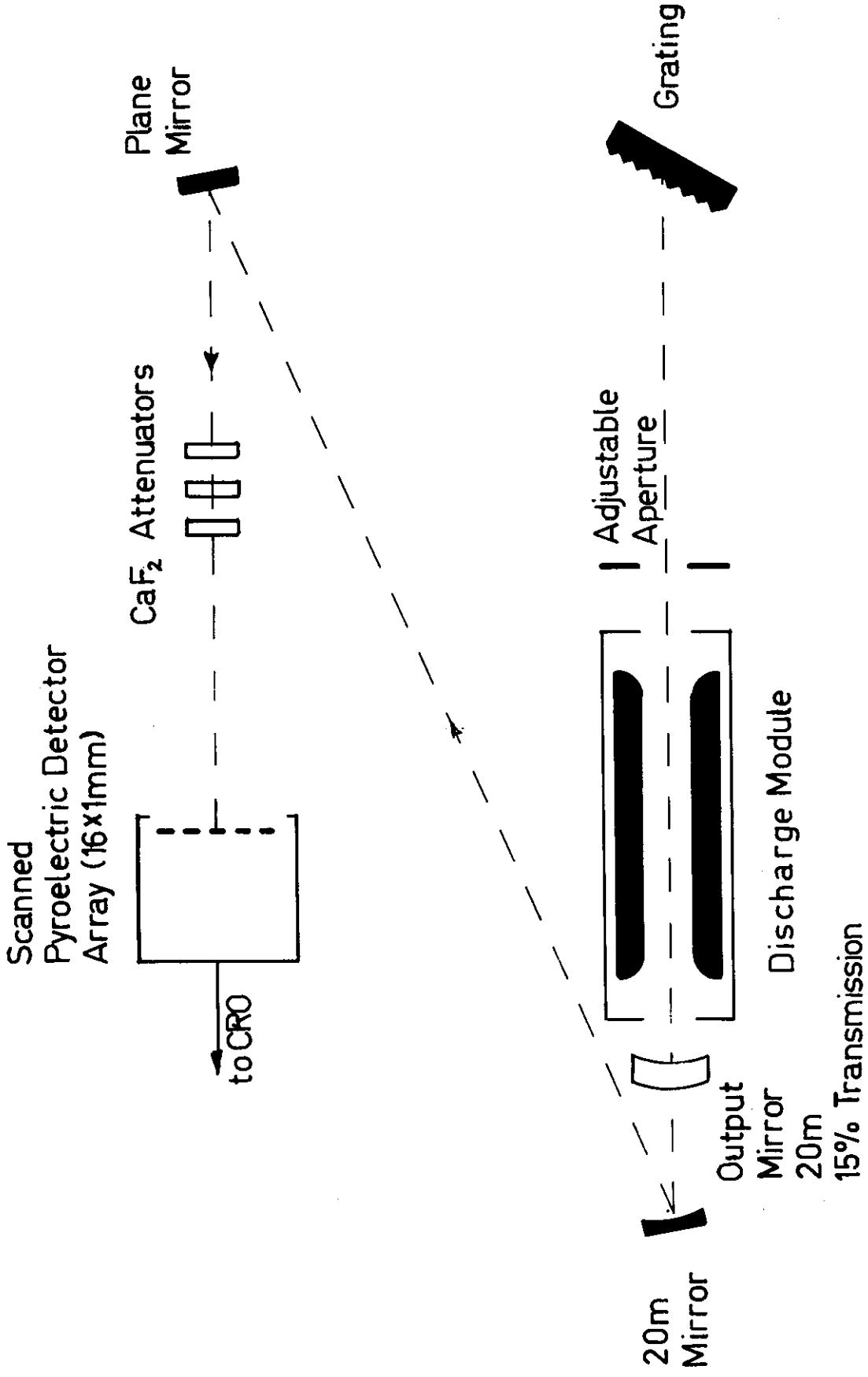


FIGURE 10. MEASUREMENT CONFIGURATION FOR FLUX DENSITY PROFILES

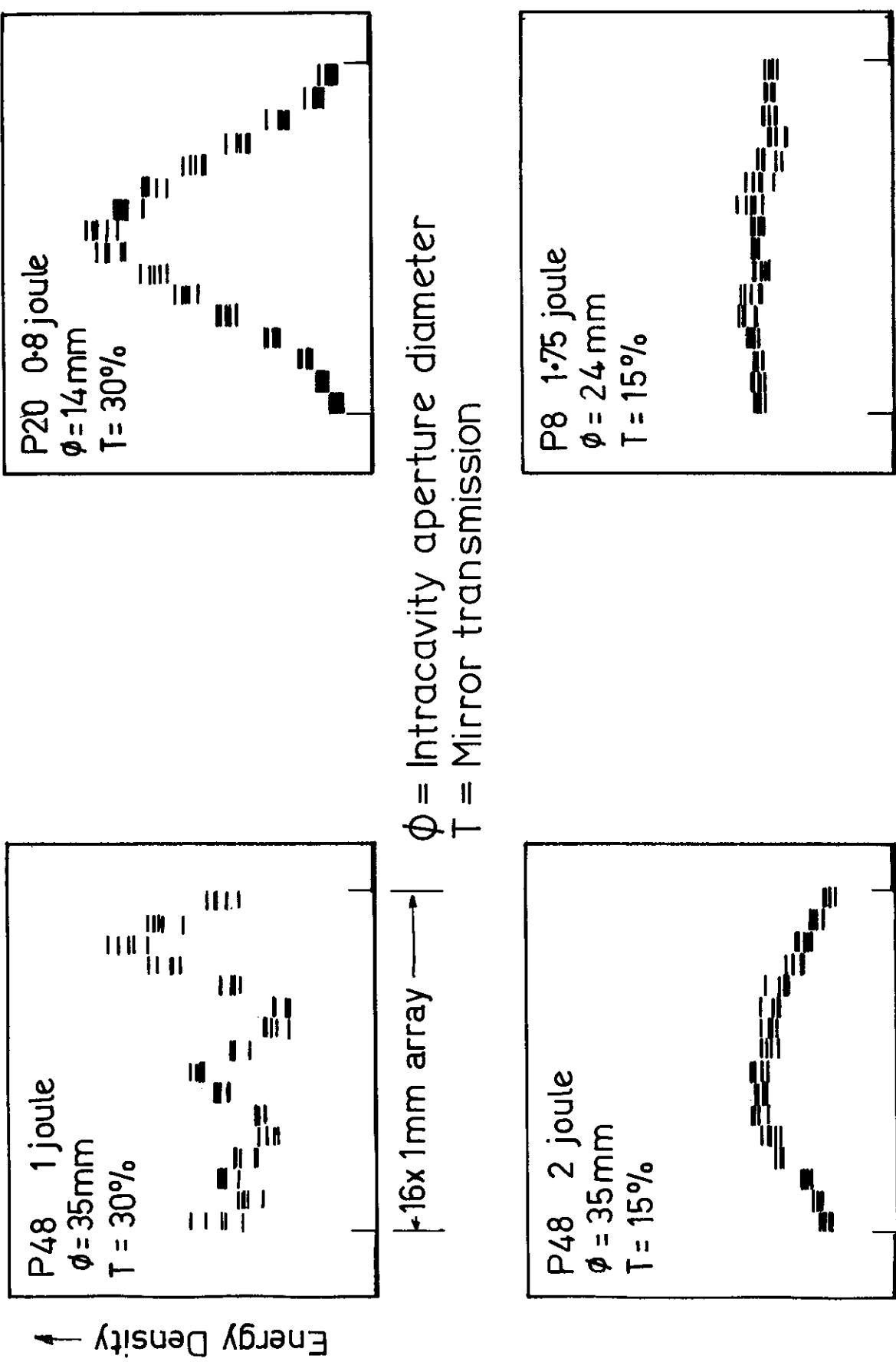


FIGURE 11. FAR FIELD FLUX DENSITY PROFILES